A STABLE PRODUCTION OF INTENSE ELECTRON BEAM PLASMA WITH ION BACK STREAM

Johshin Uramoto

IPPJ-237 Dec. 1975

Further communication about this report is to be sent to the Research Information Center, Institute of Plasma Physics, Nagoya University, Nagoya 464, Japan.

ABSTRACT

An intense electron beam is extracted without space charge limit from a dc plasma source along a magnetic field. The beam space charge is neutralized stably through back streaming of self-ionized ions from the beam extracting anode region where a neutral gas is fed locally. In Appnedix I, a space charge free electron gun is designed under this neutralization method. In Appendix II, a dynamic discharge through a series resistance is described, where an operative mechanism of the well-known TP-D plasma is clarified.

1. INTRODUCTION

In order to extract an intense electron beam from a plasma source, a space charge limit due to an electron sheath must be canceled between the extracting anode and the plasma source. One neutralizing method is due to ions ionized by the extracting electron beam itself while a neutral gas is fed into the extracting space. However, in this method, the extracting electron beam becomes unstable near the critical neutralization (the beam density $n_b \approx$ the ionized ion density n_i) as reported already by Nezlin.[1] According to that experiment, the extracting electron beam through the (cold ion) plasma has an upper limit to the current density, beyond which the extracting beam becomes unstable[2] with respect to formation of a virtual cathode. The limiting stable beam current density j_c is given by, in relation with the plasma thermal electron current density j_{th},

$$j_c \approx 0.7\, j_{th} . \qquad \cdots\cdots (1)$$

That is, the stable density condition is expressed by

$$n_b/n_e \lesssim v_e/(6\, v_b) = \frac{1}{6}\sqrt{\frac{V_e}{V_b}} , \qquad \cdots (2)$$

where $j_c = en_b v_b$ and $j_{th} = \frac{n_e v_{th}}{4}$, and n_b, v_b, V_b or n_e, v_{th}, V_e are the electron beam density, velocity, energy or the plasma thermal electron density, velocity, energy. Then, the cold ion density n_i is equal to $(n_e + n_b)$. For example V_b = 300 eV and V_e = 3 eV, we obtain $n_b/n_e \approx n_b/n_i < 1/60$

as a stable condition. Thus, the stable electron beam like plasma ($n_b \approx n_i$) is not produced by this neutralization method.

Usually, this beam unstable state transfers into a secondery discharge through some instabilities.

In this paper, a stable production of the critically neutralized electron beam ($n_b \approx n_i$) will be investigated as a development from a space charge neutralization of electron sheath due to an ion back stream. The neutralizing mechanism may be similar to a "cathode fall" in a dc discharge where the Langmuir relation $j_i/j_e \approx \sqrt{m_e/m_i}$ is satisfied (j_i, j_e; ion or electron current density and m_i, m_e; ion or electron mass). That is, their ions are beam-like.

2. SPACE CHARGE NEUTRALIZATION OF ELECTRON SHEATH

When a positive potential is applied for a diffusional plasma slab along a uniform and strong magnetic field B through a metal plate as shown in Fig.1(A), an electron sheath is produced in front of the metal plate. The potential distribution along the plasma slab will be produced as shown in Fig.1(B), if the initial velocity of the diffusional electron is neglected. Then, for neutralization of the electron sheath, we can consider two stable methods: The one method is due to a secondary discharge through a neutral gas introduction. The discharge characteristic potential distribution along B will be shown by a broken line in Fig.1(B), if the initial velocity of the source plasma electron is neglected. This neutralization does not mean $n_b \approx n_i$, but $n_b \ll n_i$).

The other method is due to ion back streams through a metal mesh plate and a differential neutral gas introduction outside of the mesh plate as shown in Fig.2(A). Because electron beams are produced in the electron sheath, which can ionize the neutral gas through the mesh. Obviously, a differential pumping for the neutral gas and the electron sheath dimension for the mesh holes must be considered. Then, if sufficient ions stream backwards along B under the ion accelerating electric field in the electron sheath, the electron sheath like potential distribution along B will be varied as shown in Fig.2(B) through a continuous neutralization due to ion streams. That is, this state may produce a constant electric field between the extracting mesh plate and the plasma source, which means a "space charge-free" state. We call this mode "electron beam mode" against "electron sheath mode" (precisely, diffusion plus sheath mode) and "discharge mode" (precisely, secondary discharge mode) in Fig.1(B).

In this electron beam mode, it should be noted that the electron beam may be extracted directly from the plasma source. Therefore, an intense current electron beam may be produced even if the initial diffusional plasma is thin. That is, in the electron beam mode, the electron current is limited by only a kind of temperature limit $n_b v_b \approx n_e v_{th}$ (where n_b, v_b and n_e, v_{th} are a density, velocity in the extracted electron beam and an electron density, thermal velocity in the plasma source), while, in the electron sheath mode, it is limited by the initial diffusion flux in relation with the sheath thickness and the applied voltage.

If these principles are considered along a sufficiently strong magnetic field and one hole of the metal plate as shown in Fig.3, the electron beam in the beam mode will concentrate within the hole area. On the other hand, in the electron sheath mode, the electron current will flow over all the metal plate area. Furthermore, in the electron beam mode, as an ion beam is injected backwards, high temperature ions may be produced through some collisions, and the ionization rate may be higher since a neutral gas is not ionized directly there.

3. EXPERIMENTAL APPARATUS

A schematic of the apparatus is shown in Fig.4. First, it should be noted that a direct damage of a hot cathode due to a secondary (high energy) ion back stream is avoided by expanding the anode space of the plasma source produced from a low voltage dc discharge. Then, the plasma source is stably operated as a secondary cathode for the extracting electron beam. Second, the electron beam extracting anode space is variable, where a neutral gas is fed locally. Third, a neutral gas pressure in each region is considered in relation with each electron-neutral mean free path. In the plasma source, the mean free path λ_1 must be shorter ($\lambda_1 \quad \ell_1$) than a distance ℓ_1 of the anode space along B in order to increase the ionization rate and to avoid the secondary ion back stream. In the beam extracting region, the mean free path λ_2 must be much longer ($\lambda_2 >> \ell_2$) than the extracting length ℓ_2 along B. However, in the extracting anode space, the mean free path λ_3 must be determined experimentally to unilize a critical ionization. We find the mean free path $\lambda_3 \approx \ell_3$ (a distance of the extracting anode space along B).

In the plasma source, a dc discharge is fired, in a helium gas, between an oxide cathode (30 mmϕ) and a couple of earthed anode with an aperture of 12 mmϕ (A_1) or 8 mmϕ (A_2). The two anodes are placed 16 cm away along a uniform magnetic field B = 2 kG.

In order to extract an electron beam from the plasma source, two extracting anodes are placed. The one extracting anode E_1 is set 40 cm away from the one plasma source anode A_2, which has an aperture of 1.5 cmϕ and a length of 2.5 cm. The other extracting anode E_2 is movable up to 16 cm along B. The helium gas (He) is fed between these two extracting anodes independently of the plasma source. These two extracting electrodes are connected to a positive dc power supply (V_E). The apparatus chamber consists of glass tubes of 10 cm in diameter. The plasma source discharge current is varied from I_d = 3.0 A to 9.0 A at the nearly constant discharge voltage $V_d \simeq 35 \sim 40$ V. Then, the extracting voltage V_E is varied up to 400 V. The initial diffusional electron current I_{EO} to the extracting anodes at the extracting voltage $V_E = 0$, must be negligibly small compared with the extracted electron beam current I_E in order to be "beam-like". Thus, the helium gas pressure P_1 at the plasma source (the cathode region and $\overline{A_1A_2}$ region) is limited below 1.4

$\times 10^{-2}$ mmHg while the direct discharge between the hot cathode and the extracting anodes, is avoided also. On the other hand, to produce a high density plasma source, the helium gas pressure must be higher. Thus, the neutral gas pressure P_1 at the plasma source ranges from 3.5×10^{-3} mmHg to 10^{-2} mmHg, which is kept at $P = 7.0 \times 10^{-3}$ mmHg usually. (A pressure between A_1 and A_2 anodes is nearly equal to the cathode region pressure at this pressure range. Therefore, we denote P_1 as a plasma source pressure). Obviously, the electron-neutral mean free path λ_1 is shorter than a distance of the source anode space $\ell_1 = 16$ cm. That is, $\lambda_1 < \ell_1$ at the plasma source.

In the beam extracting space ($\overline{A_2E_1} \equiv \ell_2 = 40$ cm), the neutral gas pressure is kept usually below 7.0×10^{-4} mmHg to avoid a secondary discharge, which is limited by the vacuum pump speeds in relation with the differential gas feeds in the plasma source and the extracting anode space. That is, $\lambda_2 >> \ell_2$, if the extracted electron beam energy is large sufficiently, where λ_2 is the electron-neutral mean free path. However, to compare with a neutralization state due to direct gas ionizations, the neutral gas is introduced above 7.0×10^{-4} mmHg into the beam extracting space (from a gas port (C1) as shown in Fig.4). A neutral gas pressure at the extracting anode space ($\overline{E_1E_2} \equiv \ell_3 \lesssim 16$ cm) is determined experimentally, where the electron-neutral mean free path λ_3 may be comparable with ℓ_3. That is, $\lambda_3 \approx \ell_3$.

Under these pressure conditions, a positive voltage

V_E is applied to the beam extracting anodes E_1 and E_2 for the earthed plasma source anodes A_1 and A_2.

4. EXPERIMENTAL RESEARCH

First, the neutral gas is directly introduced into the beam extracting space between E_1 and A_2 at the collector (E_2) posistion 1 (C1) without the extracting anode space as shown in Fig.4, while a positive voltage is applied to the extracting anodes at V_E = 300 V. Dependences of the total electron current I_E and the collector current I_C on the $\overline{E_1A_2}$ region pressure P_2 are shown in Fig.5(A). Then, an unstable electron current fluctuation appears in some narrow pressure region, whose period is about a few milli-seconds as demonstrated by Nezlin's experiment[1]. This un-stable current state transfers into a secondary discharge abruptly. That is, a stable current peak does not appear in this case.

Next, the neutral gas is fed between E_1 and E_2 at the collector position 2 (C2) (the beam extracting anode space is very wide and long along B). Under V_E = 300 V, dependences of the total current and the collector current on the $\overline{E_1E_2}$ region pressure P_3 are shown in Fig.5(B), while the extracting space $\overline{E_1A_2}$ region pressure is kept constant almost. Obviously, each electron current increases abruptly with the pressure P_3 up to a peak value. It should be remarkable that the peak current is very stable compared with a case of the collector position 1. Moreover, a difference of electron current behavior between the two cases of the collector position should be noted for the (central) collector current I_c: The electron current peak at the collector position 2 concentrates in the central hole region at about 90 %, while the corresponding electron collector current at the collector position 1 is below 40 %. We can consider that the peak electron current at the collector position 2 is extracted from the plasma source. Because the initial diffusion current at the extracting voltage $V_E = 0$ is negligibly small compared with the peak current, and the pressure P_2 in the extracting space is not varied almost effectively. Also, an electron current conservation is observed as $I_d = I_E + I_S$ where I_d, I_E and I_S are the total discharge current, the extracted total electron current and an electron current to the plasma source anodes A_1, A_2.

The peak currents under the variable pressure P_3 are independent of the extracting voltage V_E for $V_E > 40$ V (above the discharge voltage or the helium ionization voltage) as shown in Fig.6, which depends on the discharge current I_d and the neutral gas pressure P_1 at the plasma source. These facts mean that the peak currents under the variable pressure P_3 are limited by the source electron flux $n_e v_{th} \Delta S$ (a kind of temperature limit), where n_e, v_{th} and ΔS are an electron density, thermal velocity and the source anode hole (in A_2) area. On the other hand, the stable electron current at the collector position 1 will be limited by the diffusional current as compared also in Fig.6. The peak or maximum electron current I_{CM} to the collector at the collector position 2 (C2) increases quickly with the source discharge current I_d as shown in Fig.7, while the diffusional limited current I_{CS} at the collector position 1 (C1) increases slowly. A ratio (I_{CM}/I_d) between the maximum collector current at (C2) and the source discharge current depends on only the source pressure P_1 and varies from 10 % to 30 % for $3.5 \times 10^{-3} < P_1 < 10^{-2}$ mmHg. Usually, the ratio I_{CM}/I_d is about 15 % at a standard pressure $P_1 = 7.0 \times 10^{-3}$ mmHg. Similarly, the diffusional limited current I_{CS} at (C1) increases with P_1.

When the collector E_2 is moved and a distance ℓ along B of the extracting anode space is varied at $V_E = 400$ V, the maximum collector current I_{CM} varies with a neutral gas pressure which gives the maximum collector current. Dependence of I_{CM} on ℓ are shown in Fig.8 with the pressure P_3. Obviously, the maximum collector current decreases and becomes unstable when the distance ℓ decreases. It should be emphasized that the distance ℓ along B is essential for a stability of the maximum electron beam current even if the pressure (P_3) is corrected highly.

5. DISCUSSION

The mode transition for an electron sheath mode, beam mode and a secondary discharge mode as described in section 2, is investigated, while the movable corrector E_2 is fixed at the collector position 2 (with the wide anode space) and the pressure P_2 is varied through P_3 (gas port C2). A total electron current I_E for $V_E = 300$ V or 0 to the extracting anodes is shown in Fig.9, while the neutral gas pressure P_2 in the beam extracting space $\overline{A_2E_1}$ is monitored. For the various P_2, three typical radial distributions of the plasma wall potential at the median plane between E_1 and A_2 are shown in Fig.10. Obviously, these distributions correspond to the electron sheath mode, electron beam mode and secondary discharge mode as described above. The current concentrations to the central region are shown in Fig.11 by a ratio between the collector current I_C and the total current I_E. The radial ion saturation current distributions corresponding to their three modes are shown in Fig.12. In the sheath mode, the radial ion relative density distribution is broad. Next, the corresponding Langmuir probe characteristics are shown in Fig.13 near the glass chamber wall. Then, in the beam mode, the plasma near the wall is very ion-rich. This ion rich effect in the beam mode is related also with the plasma wall potential as shown in Fig.10 near the chamber wall. The maximum plasma wall potentials V_M normalized by the beam extracting voltage V_E is shown in Fig.14 for V_E. It should be noted that the maximum wall potential is up to twice of V_E. These high positive potential may be due to the ion beams inversely accelerated under the electric field extracting the electron beam. Meanwhile, an ion heating may occur through some collisions. In fact, the Langmuir probe characteristic of the beam mode as shown in Fig.13 denotes a presence of high temperature ion ($\sim$ 100 eV).

In this beam mode, the electron density n_b is estimated from the extracted beam current density and an averaged energy which may be expressed by $\bar{V} = \sqrt{V_E \cdot V_d}$, where V_d is the discharge voltage corresponding to the initial energy. That is,

$$n_b \approx I_c / (e \bar{v}_b S) , \quad \cdots\cdots\cdots (3)$$

where I_c, $\bar{v}_b$ and S are the collector electron current, the mean electron velocity ($= 5.9 \times 10^7 \sqrt{\bar{V}}$ cm/sec) and the beam cross-section (the hole area in A_2 anode). For $V_E = 300$ V, $V_d \approx 35$ V and $I_c \approx 1.0$ A, we obtain $n_b \approx 3 \times 10^{10}$/cc from $S \approx 0.5$ cm^2. On the other hand, the corresponding ion density n_i may be estimated from Bohm formula[1] using an ion saturation current as shown in Fig.12 and an electron temperature (about 80 eV near the central beam column). We obtain $n_i \approx 5 \times 10^{10}$/cc for the collector current I_c = 1.0 A at $V_E = 300$ V. Then, we find that $n_b \approx n_i$ is satisfied nearly.

In the plasma source, the electron density n_e and the electron temperature V_e of the central plasma column is about $n_e \approx 4 \times 10^{11}$/cc and $V_e \approx 5$ eV when $I_d \approx 5.0$ A and $P_1 \approx 7.0 \times 10^{-3}$ mmHg at the beam mode. Thus, we find a kind of temperature limit $n_b \bar{v}_b \approx n_e v_{th}$ is roughly satisfied, where v_{th} is a thermal electron velocity in the plasma source. THe current limit extracted from the plasma source may be estimated from a ratio $(d_A/d_K)^2 \approx 0.16$ between the discharge anode hole area $\pi\ (d_A/2)^2$ and the oxide cathode surface area $\pi\ (d_K/2)^2$ where $d_A = 12\phi$ and $d_K = 30\phi$. That is, $I_E/I_d \approx I_c/I_d \approx (d_A/d_K)^2 \approx 0.16$ at the beam mode. In this estimation, it is assumed that the oxide cathode electron emission is uniform all over the diameter (30 ϕ). When the oxide coat in the central area of the cathode is removed and retained only outside of the cathode surface, we find experimentally that (I_c/I_d) decreases abruptly. That is, the electron emission from the central region of the cathode is very important to extract the intense electron beam.

The normalized ion density fluctuation $\delta n/n$ is investigated in Fig.15. Then, we find that the plasma in the extracting space is most quiescent in the beam mode. This phenomena may be explained from a canceling effect of electron space charge oscillations due to back streaming ions. This fact may be related with a quiescent plasma (ion) heating method, while the ordinary cross-field heating or wave heating is very noisy.

Furthermore, it should be pointed out that a highly ionized plasma may be produced because a neutral gas does not introduce directly for the ionizations.

This neutralized beam described here, may be compared with an ordinary hollow anode discharge. However, that hollow anode discharge voltage is kept almost near the cathode, where the plasma is a "positive column" due to a beam discharge in a neutral gas. Moreover, that discharge voltage is low and "uncontrolable". On the other hand, in our case, the beam plasma is not a positive column due to a discharge, but a developed or technical "cathode fall" whose voltage is "controllable". The essential differences between the ordinary hollow anode discharge and our case may lie in the distance of the extracting anode space along

B under the differential pumping, and in the independent plasma source.

Besides, this paper beam mode must be distinguished from the case that a positive potential from the end target is applied[3] to a dc plasma coming along B (for example, PIG plasma). That potential application from the end produces an electron sheath (mode) with an initial velocity effect or a secondary discharge.

6. CONCLUSION

A space charge free stable electron beam is extracted directly from a dc discharge plasma source along a strong magnetic field, while ions stream backwards through a local neutral gas feed into the beam extracting anode space.

ACKNOWLEDGMENT

I wish to thank Drs. T. Kuroda and M. Masuzaki for valuable comments.

REFERENCES

1. M. V. Nezlin, Zh. Eksp. Teor. Fiz. 41, 1015 (1961); Sov. Phys. JETP 14, 723 (1962)

2. S. Nagao et al., Ann. Rev. of IPP Japan, Apr. 1967 - Mar. 1968, p.10

3. T. Kuroda, private communication.

4. L. Brillouin, Phys. Rev. 67, 260 (1945)

5. M. Otsuka et al., Ann. Rev. of IPP Japan, Apr. 1968 - Mar. 1969, p.56

FIGURE CAPTIONS

Fig.1. (A) Electron sheath mode for diffusional plasma. B: uniform magnetic field. V_E: positive voltage. (B) Potential distributions along B. V_P: plasma potential. z: distance along B. (1): plasma potential distribution of electron sheath mode. (2): plasma potential distribution of secondary discharge mode.

Fig.2. (A) Electron beam mode with ion back streams. (B) Plasma potential distribution of electron beam mode.

Fig.3. Electron beam mode of one hole along strong magnetic field.

Fig.4. Schematic diagram of apparatus. A_1, A_2: plasma source anodes. K: hot cathode. E_1: a beam extracting anode. E_2: a movable beam extracting anode (beam collector). C1: collector position 1 (without extracting anode space). C2: collector position 2 (with wide extracting anode space). P_r: movable cylindrical probe. V_E: extracting voltage. V_d: plasma source discharge voltage. P_1, P_2, P_3: helium pressures. B: uniform magnetic field (2 kG).

Fig.5. (A) Dependences of total extracted current I_E and collector current I_c on $\overline{E_1A_2}$ region pressure P_2. Collector position C1. V_E = 300 V. I_d = 5.5 A. (plasma source pressure $P_1 = 7.0 \times 10^{-3}$ mmHg. B = 2 kG. $V_d \approx -35$ V.)

(B) Dependences of total extracted current I_E and collector current I_c on $\overline{E_1E_2}$ region pressure P_3. Collector position C2. V_E = 300 V. I_d = 5.5 A.

Fig.6. Dependences of maximum collector current I_{CM} at (C2) and saturated collector current I_{CS} at (C1) on V_E. (C1): collector position 1. (C2): collector position 2. V_E: extracting voltage. I_d = 5.5 A. $P_1 = 7.0 \times 10^{-3}$ mmHg (source pressure).

Fig.7. Dependence of I_{CM} and I_{CS} on discharge current I_d. I_{CM}: maximum collector current at collector position 2. I_{CS}: saturated collector current at collector position 1. V_E = 300 V. $P_1 = 7.0 \times 10^{-3}$ mmHg.

Fig.8. Dependence of maximum collector current I_{CM} on distance ℓ along B of extracting anode space. P_{3M}: pressure corresponding to maximum collector current. V_E = 400 V. $P_1 \approx 6.0 \times 10^{-3}$ mmHg. I_d = 9.0 A.

Fig.9. Variation of total current I_E at (C2) for $\overline{E_1A_2}$ region pressure P_2 while gas is fed from $\overline{E_1E_2}$ region. C2: collector position 2. V_E = 300 V or 0 V. $P_1 = 10^{-2}$ mmHg. $I_d \approx$ 5.0 A.

Fig.10. Radial distributions of plasma wall potential V_W for three typical modes (corresponding to Fig.9). At median plane between E_1 and A_2. (I): Sheath mode $P_2 \approx 5.2 \times 10^{-4}$ mmHg. (II): Beam mode $P_2 \approx 9.5 \times 10^{-4}$ mmHg. (III): Discharge mode $P_2 = 1.4 \times 10^{-3}$ mmHg. V_E = 300 V. I_d = 5.0 A. $P_1 = 10^{-2}$ mmHg. r: radius.

Fig.11. Current concentration to the central region (corresponding to Fig.9). (I_c/I_E): a ratio between collector current (at C2) and total current. V_E = 300 V. I_d = 5.0 A. $P_1 = 10^{-2}$ mmHg.

Fig.12. Normalized radial ion density distributions corresponding to three modes. By probe with negative bias voltage -300 V. (I): Sheath mode. (II): Beam mode. (III): Discharge mode. $P_1 = 10^{-2}$ mmHg. V_E = 300 V. I_d = 5.0 A. (i/i_o): normalized ion density.

Fig.13. Three typical Langmuir probe characteristics near chamber wall ($r \approx 4.0$ cm). (I): Sheath mode. (II): Beam mode. (III): Discharge mode. V_p: probe voltage. I_e: electron current. I_i: ion current. $P_1 = 10^{-2}$ mmHg. V_E = 300 V. I_d = 5.0 A.

Fig.14. Normalized maximum plasma wall potential (V_M/V_E) near chamber wall. $P_1 = 10^{-2}$ mmHg. I_d = 5.0 A. (I): Sheath mode. (II): Beam mode. V_M: maximum plasma wall potential. V_E: extracting voltage.

Fig.15. Variation of normalized ion density fluctuation $(\delta n/n)$ for pressure P_2 (corresponding to Fig.9). V_E = 300 V. I_d = 5.0 A. $P_1 = 10^{-2}$ mmHg.

Fig.16. Electron beam extraction to high vacuum side (Appendix I). E_3: third extracting electrode. I_b: electron beam current. (see Fig.4).

Fig.17. "Dynamic" discharge through a series resistance (Appendix II). R: variable resistance. V_o: voltage of power supply. (see Figs.4 and 16).

APPENDIX I

Space Charge Free Electron Gun

As a development of this paper, a "space charge free electron gun" is designed as shown in Fig.16. A vacuum pump is added to the experimental apparatus in Fig.4. Thus, under the beam mode operation as described in this paper, an electron beam is extracted in a high vacuum side (low pressure).

Then, a collision effect with ions is negligible usually. Because the electron-ion mean free path λ_{ei} in the $\overline{E_1E_2}$ region is sufficiently long compared with the apparatus dimensions. That is, even if the electron beam energy $V_b \approx 10^3$ eV and the density $n_b \approx 10^{13}$/cc, we obtain $\lambda_{ei} \approx 3.0 \times 10^5$ cm (from $\lambda_{ei} \approx 3.5 \times 10^{12} V_b^2/n_b$).

On the other hand, another collision effect with neutral particles will be neglected also. Because, even if the electron-neutral mean free path λ_{en} in the $\overline{E_1E_2}$ region is above 2ℓ, the neutralization mechanism is operated as found in this paper, where ℓ is a distance along B of the $\overline{E_1E_2}$ region. From another stand point, the beam mode is operated by a critical ionization in the $\overline{E_1E_2}$ region. Therefore, the electron beam component is not lost (before the beam discharge).

From these considerations, the electron beam maximum current I_b will be limited by only a Brillouin-flow[4]

$$I_b = 1.45 \times 10^{-6} r_b^2 B^2 \sqrt{V_b} ,$$

where r_b is the beam radius (cm), and B or V_b is measured by gauss or electron volt.

Experimentally, we extract as an electron beam above 10% of the source discharge current I_d in the high vacuum side ($\lesssim 10^{-4}$ mmHg) with an energy spread 20% (at V_E = 400 V and B = 2 kG).

APPENDIX II

Dynamic Discharge Operation

The electron beam as described in this paper can be produced by one power supply through a resistance load discharge as shown in Fig.17 we call "Dynamic Discharge". There, a relative extracting voltage V_E is automatically applied to the source plasma by the source anode (A_1 and A_2) current I_S passing through the series resistance R. That is, $V_E = RI_S$. The beam energy and current are adjusted by setting R and the source discharge current I_d. If the total extracted beam current I_E is given by $I_E = \alpha I_d$ (usually, in our case, $\alpha = 0.15 \sim 0.3$), we can determine $I_S = (1 - \alpha)I_d$ and $V_E = R(1 - \alpha)I_d$. Then, the power supply voltage V_o is determined by $V_o = V_d + V_E = V_d + R(1 - \alpha)I_d$ where V_d is the primary discharge voltage ($35 \sim 40$ volt, experimentally).

When the pressure in the $\overline{A_2E_1}$ region increases, a secondary dishcarge (discharge mode as described already) occurs if $V_E = RI_S$ is above the gas ionization potential. This mechanism will be equal to an operative mechanism of the well known TP-D plasma[5]. That is, the author considers that the floating electrode is earthed by an effective low resistance ΔR through a narrow gap to the earthed anode. Thus, initially, a primary dishcarge current I_d flows (by-passes) through this effective series resistance ΔR between the anode and the floating electrode. Next, by this current load $I_d \Delta R$, a secodary discharge starts between the anode and the floating electrode if the gas pressure is higher. Obviously, $I_d \Delta R$ must be higher than the helium ionization potential (24.5 V). If the neutral gas pressure between the anode and the floating electrode decreases below a critical value, the secondary discharge stops and the resistance load voltage $I_d \Delta R$ is applied to a diffusional plasma flow from the primary discharge (cathode) region. Thus, an electron sheath mode as described already will appear. It should be noted that the effective resistance ΔR may depend on the local plasma density and may be uncontrollable externally. If the distance between the anode and the floating electrode increases and the floating electrode is earthed through a fixed resistance R, the demerit will be avoided.

In the TP-D plasma, the diffusional plasma density from the primary discharge decreases abruptly through neutral collisions along B because of the high pressure ($>$ 0.2 mmHg) operation. Therefore, the secondary discharge is essential to obtain a high density plasma in the "test plasma region", while the ionization rate decreases. Even if many floating electrodes are used, these principles will be applied.

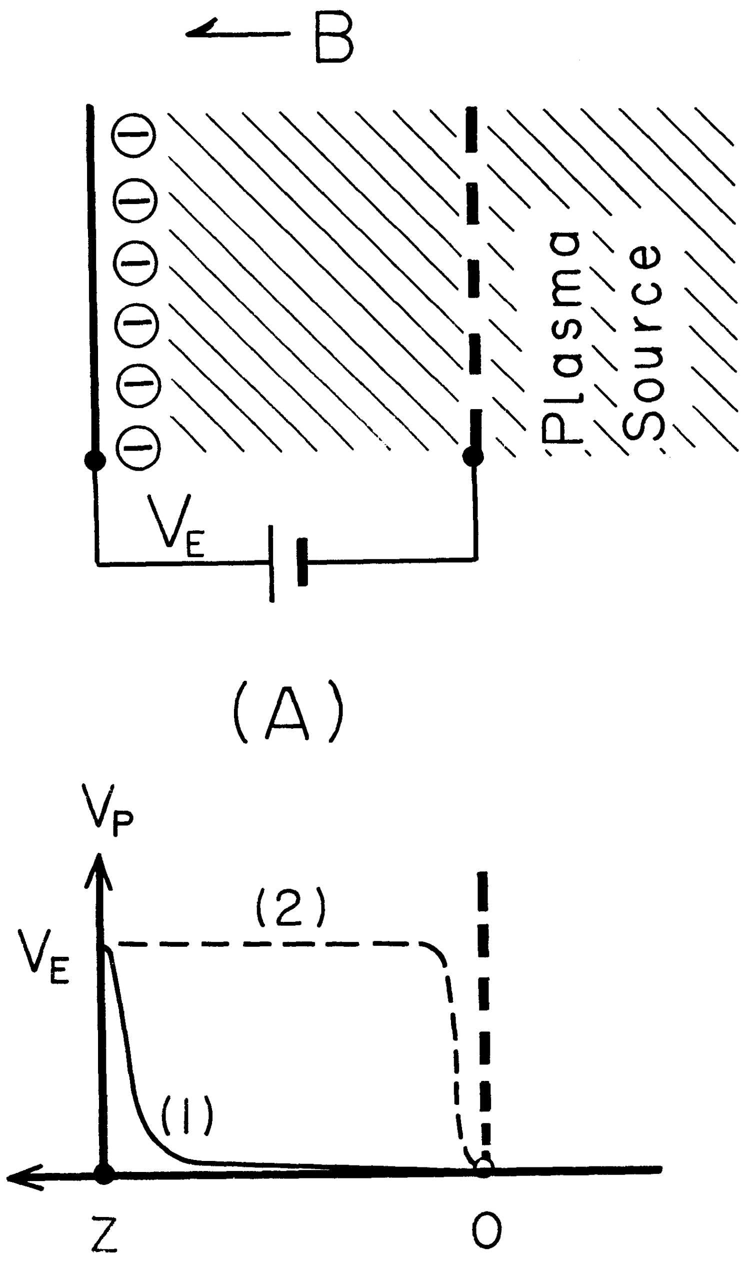

Fig. 1

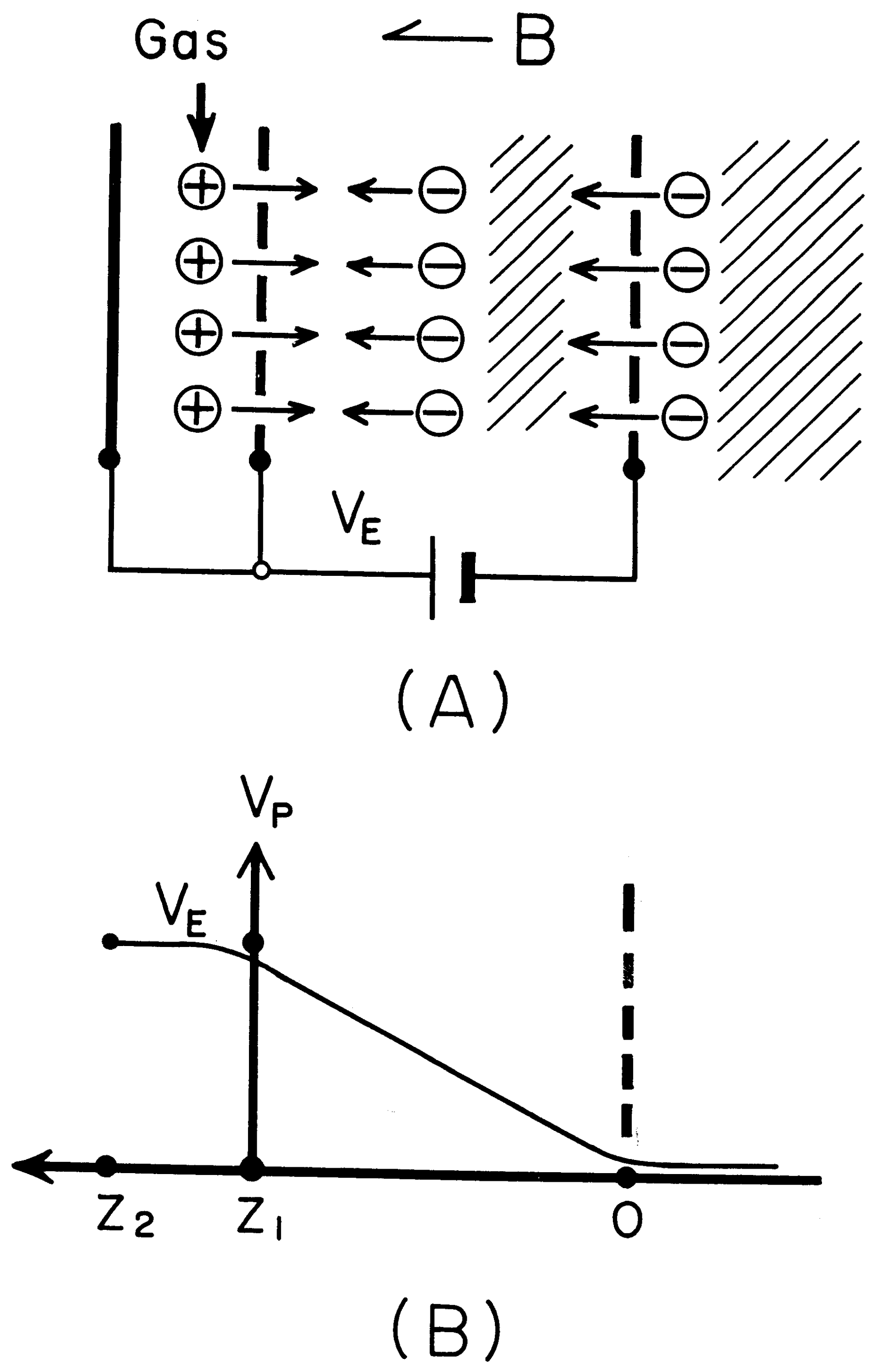

Fig. 2

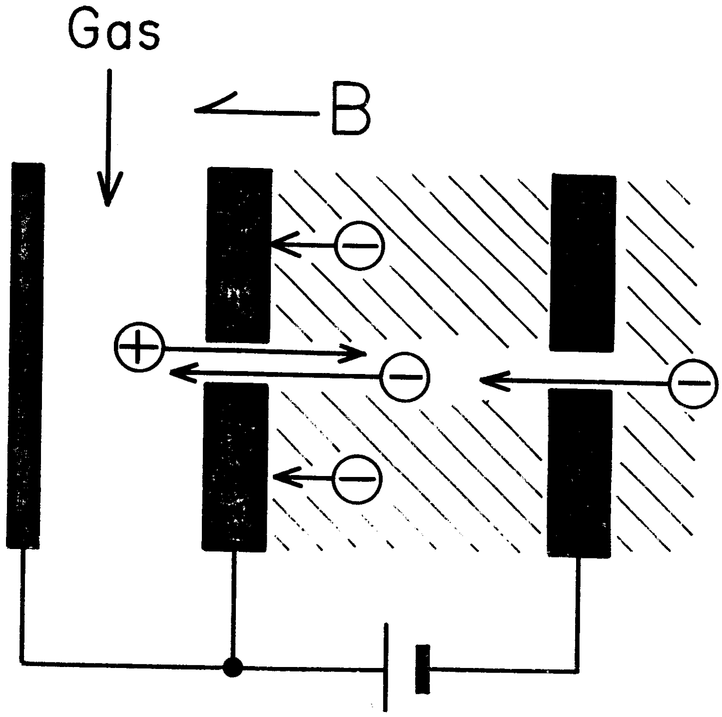

Fig. 3

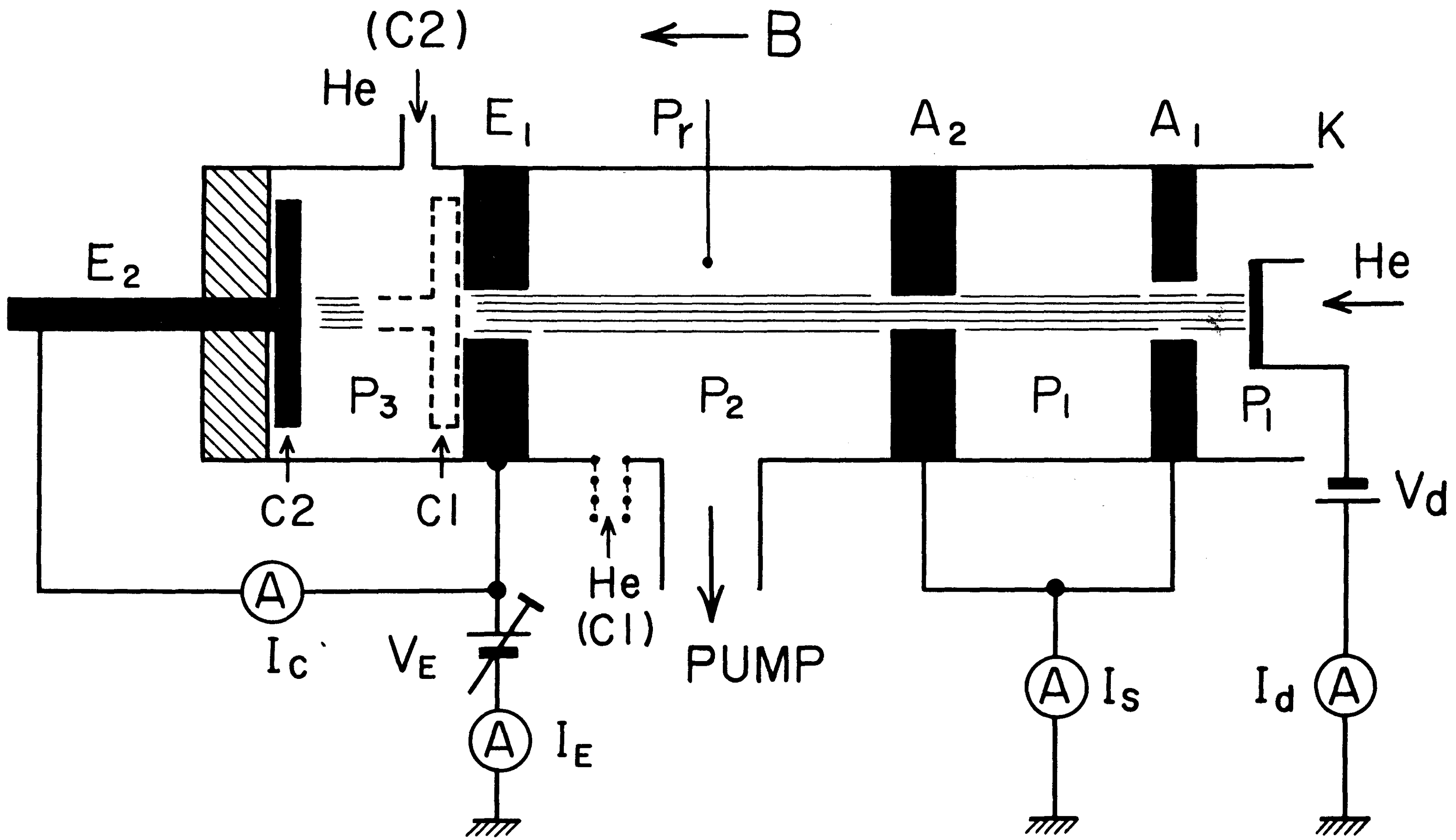

(C2)
B
He
E1
Pr
A2
A1
K
E2
He
P3
P2
P1
P1
C2
C1
Vd
He
(C1)
A
Ic
VE
PUMP
A
Is
Id
A
A
IE

Fig. 4

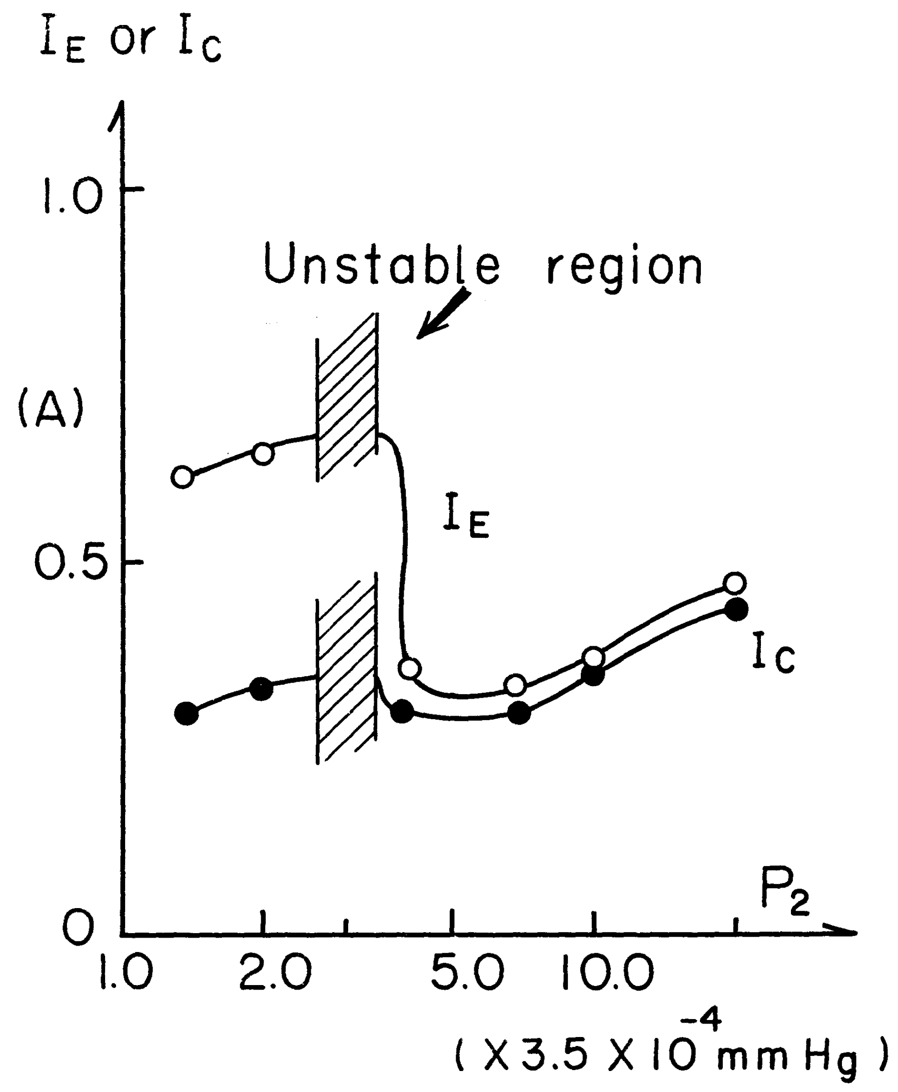

I_E or I_C
1.0
(A)
0.5
0
Unstable region
I_E
I_C
P_2
1.0
2.0
5.0
10.0
(X 3.5 X 10^{-4} mm Hg)

Fig.5 (A)

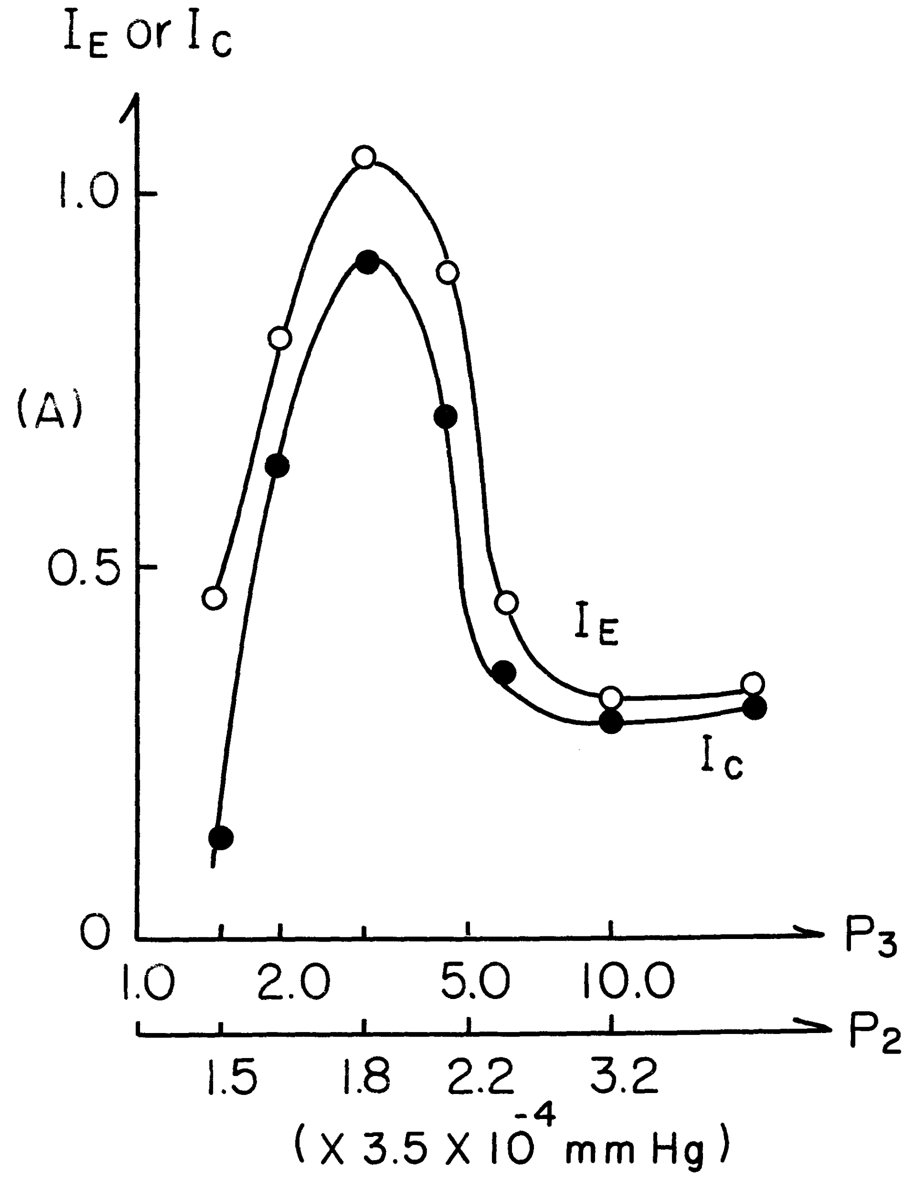

Fig.5 (B)

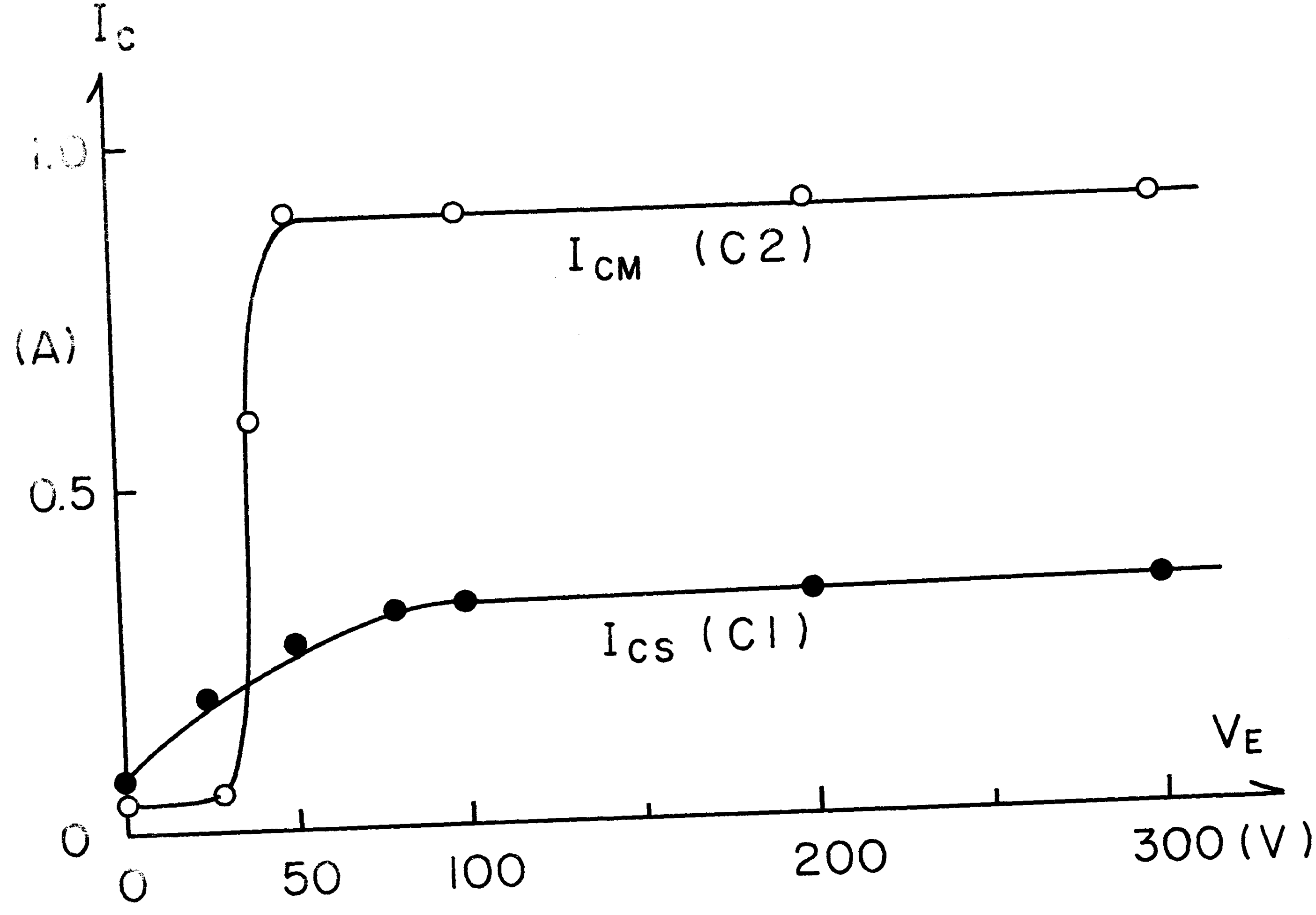

Fig. 6

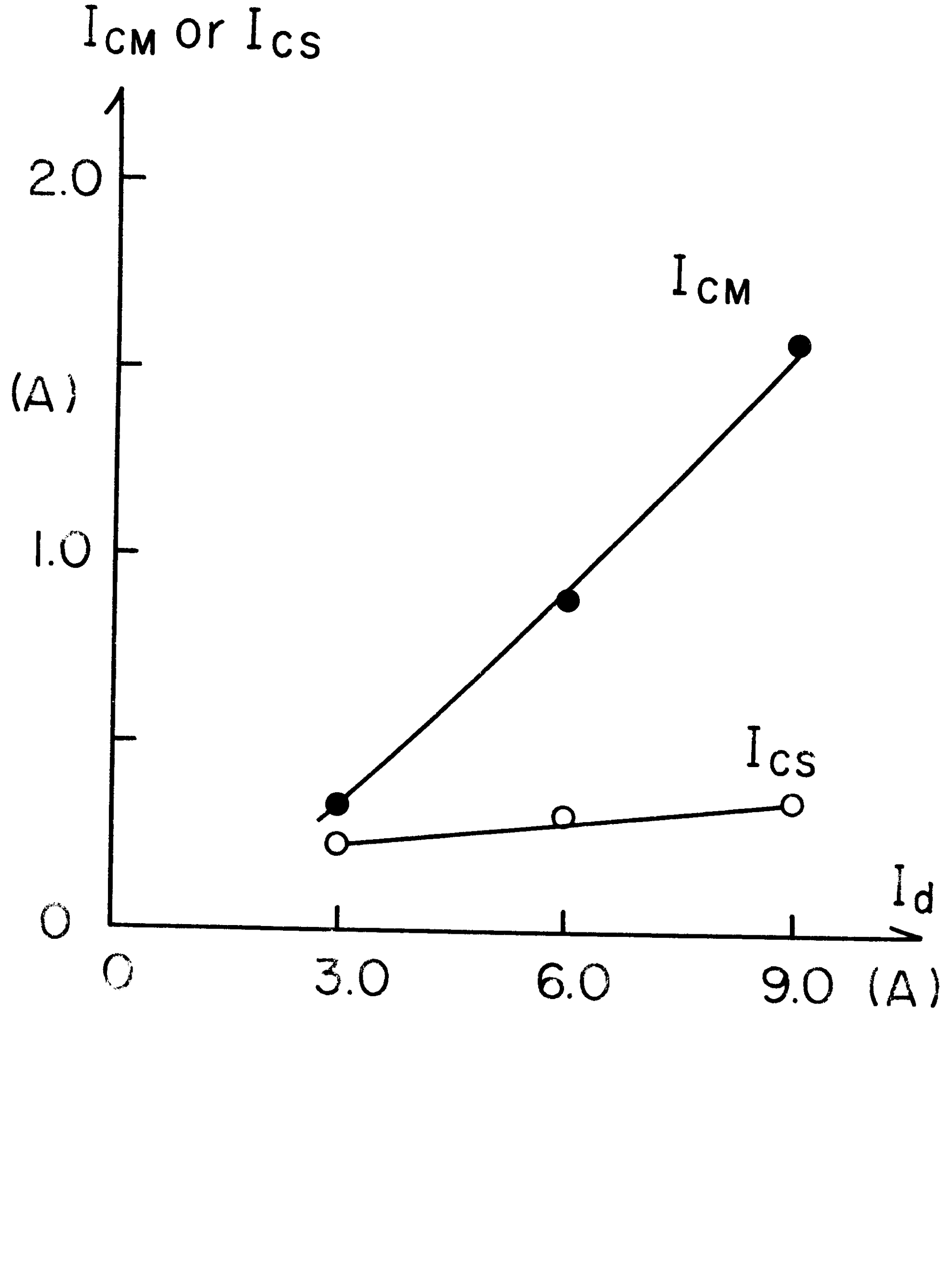

Fig. 7

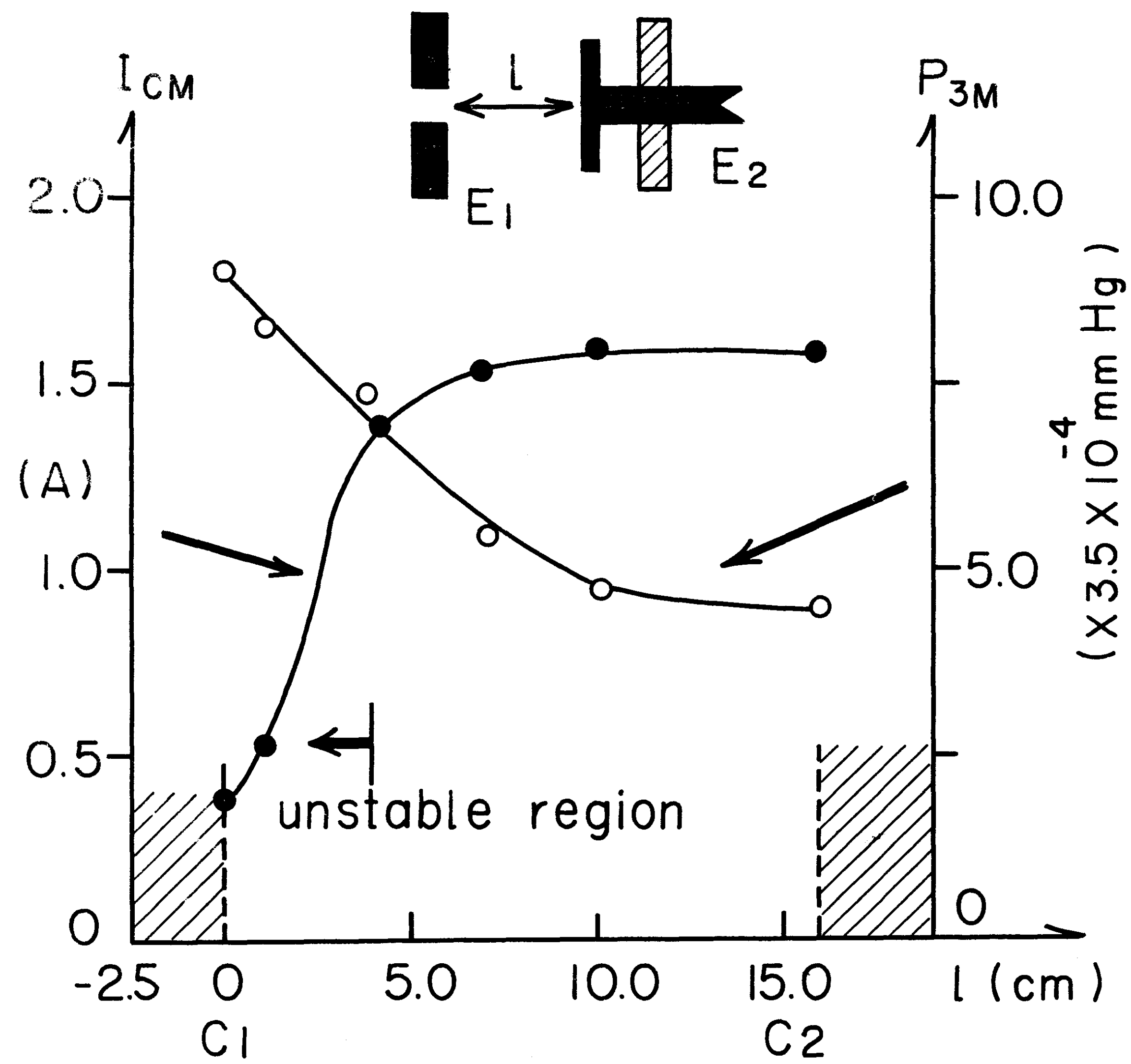
I CM
(A)
2.0
1.5
1.0
0.5
0
-2.5
0
5.0
10.0
15.0
C1
C2
l (cm)
P 3M
10.0
5.0
0
(X 3.5 X 10 -4 mm Hg)
E1
E2
l
unstable region

Fig. 8

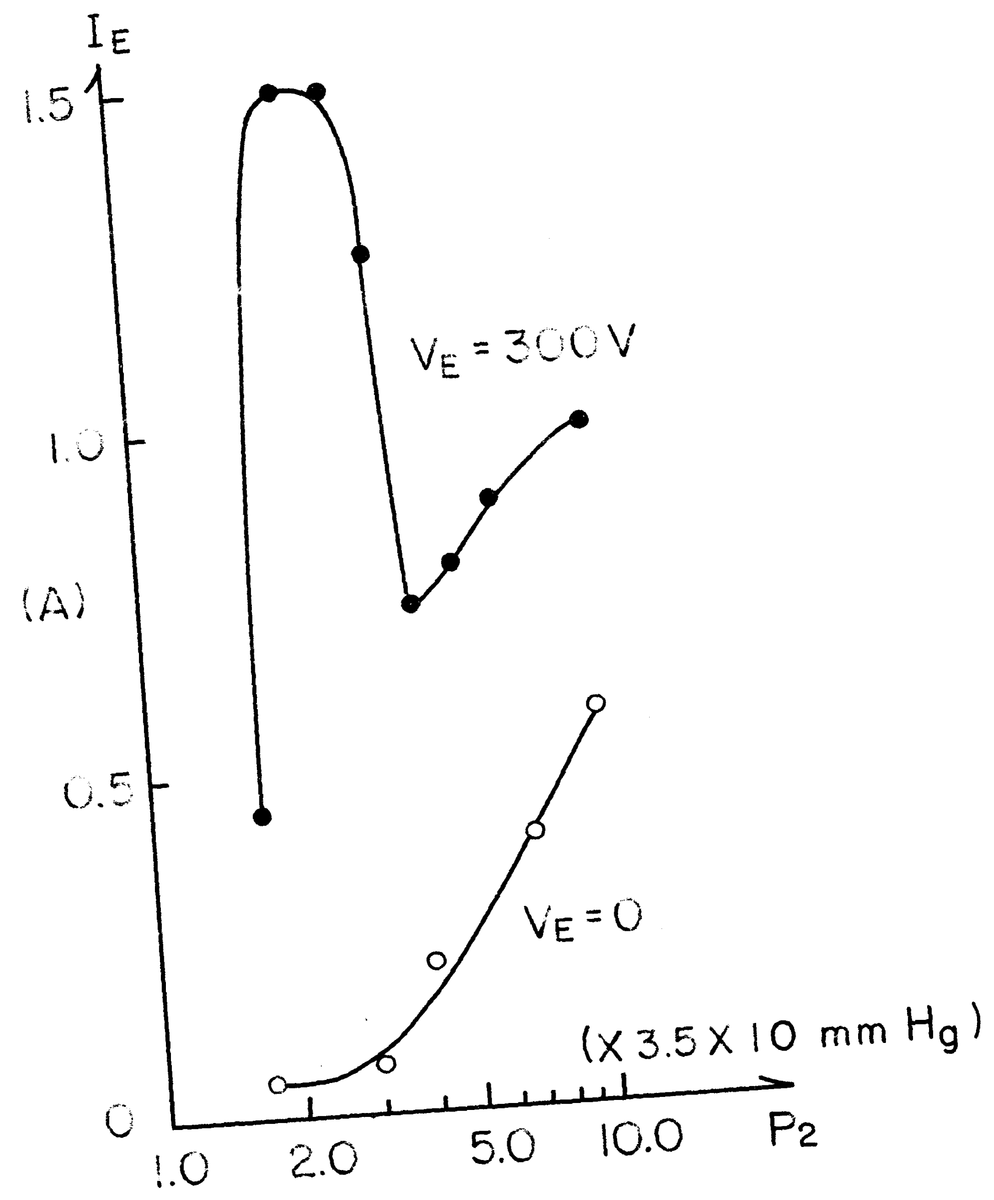

Fig. 9

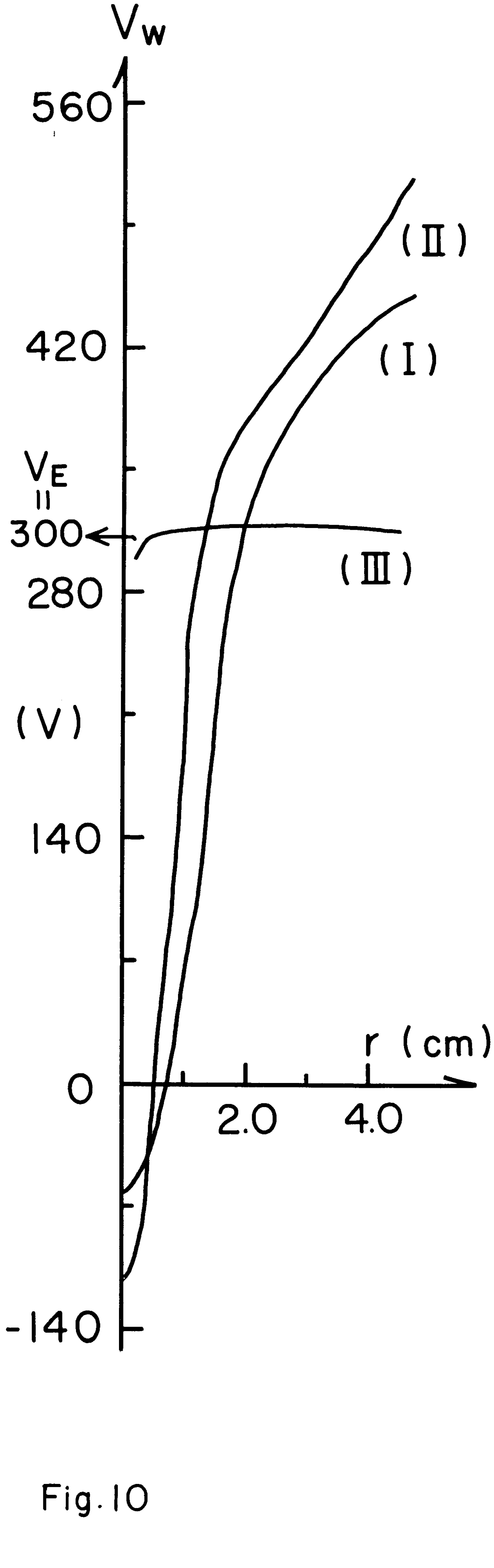

Fig. 10

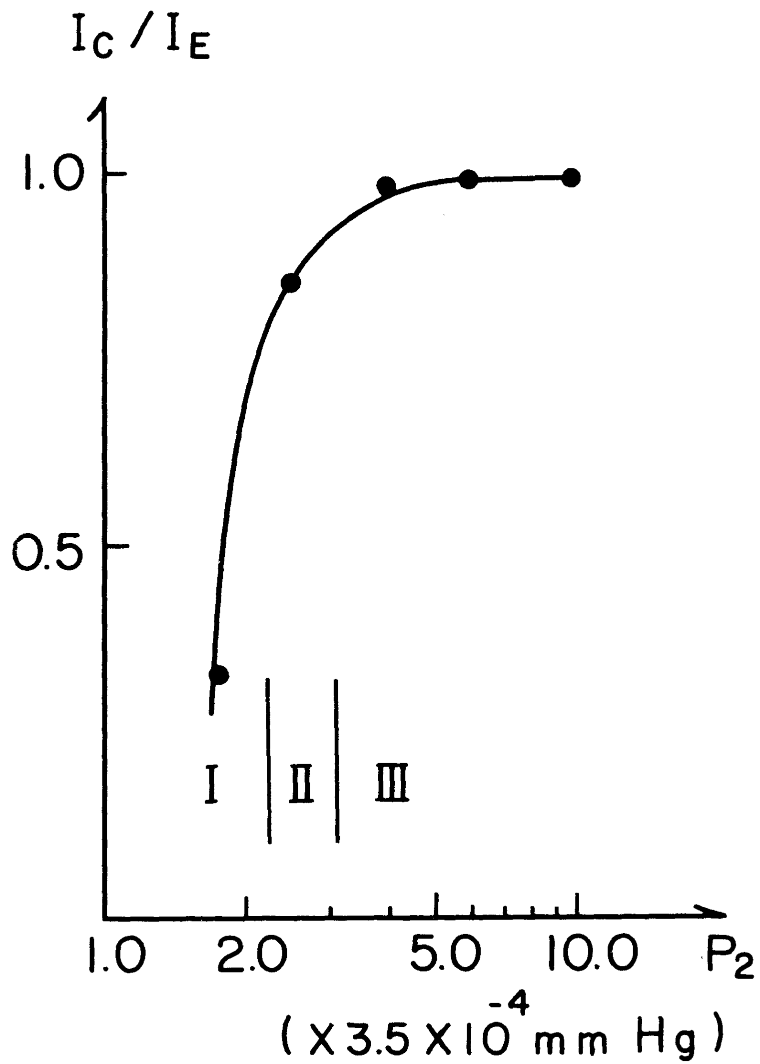

Fig. 11

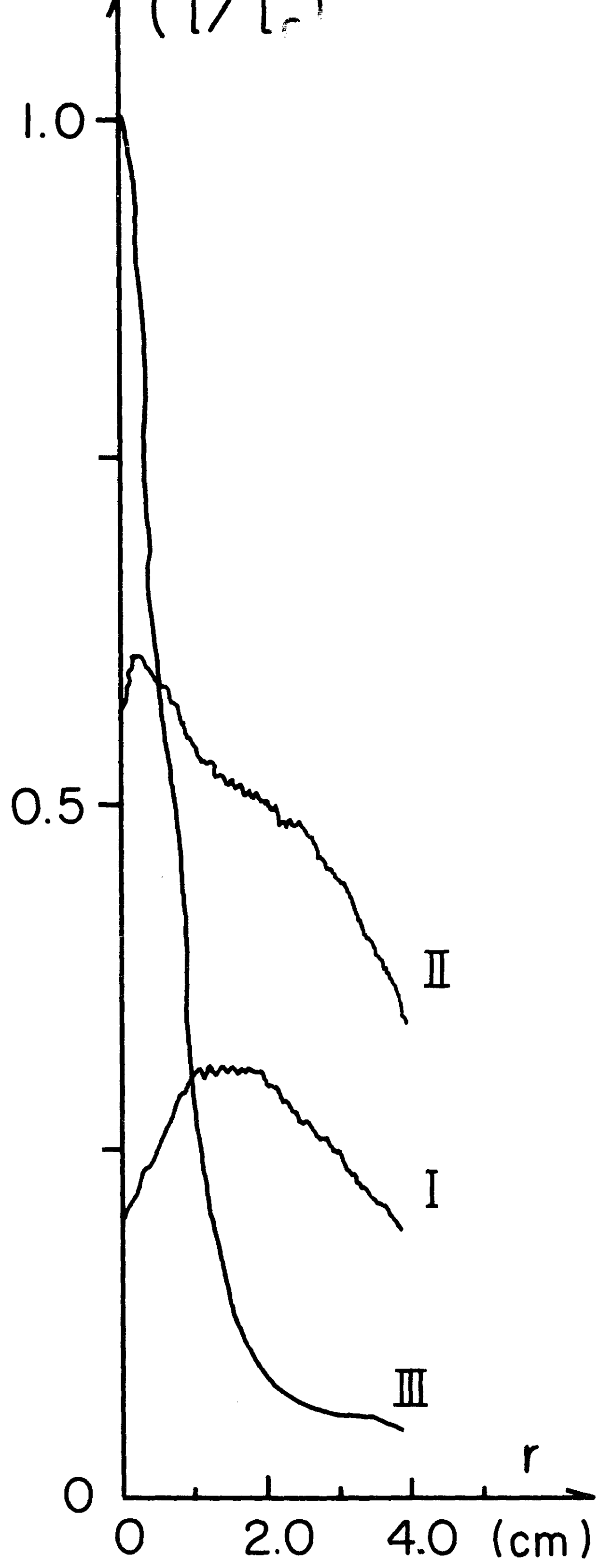

Fig.12

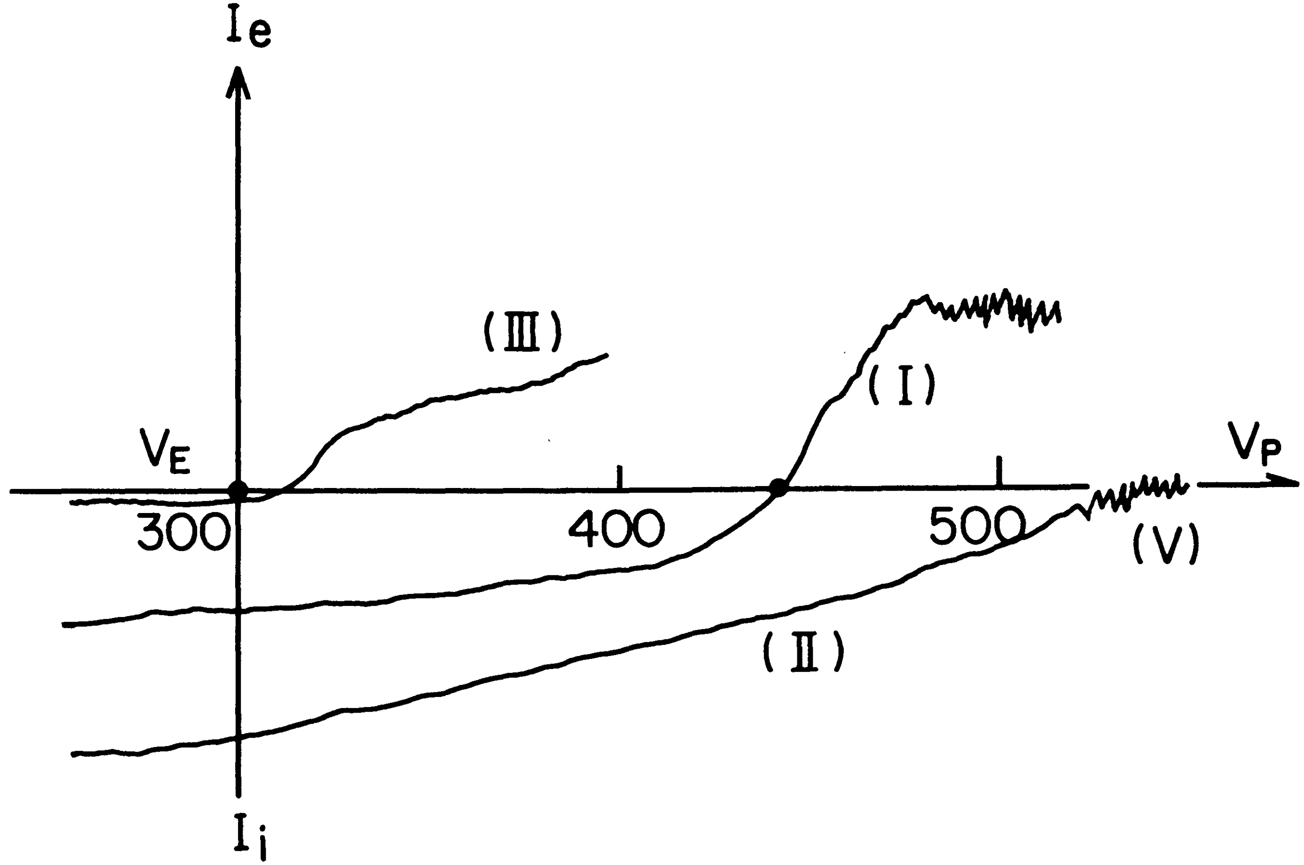

Fig. 13

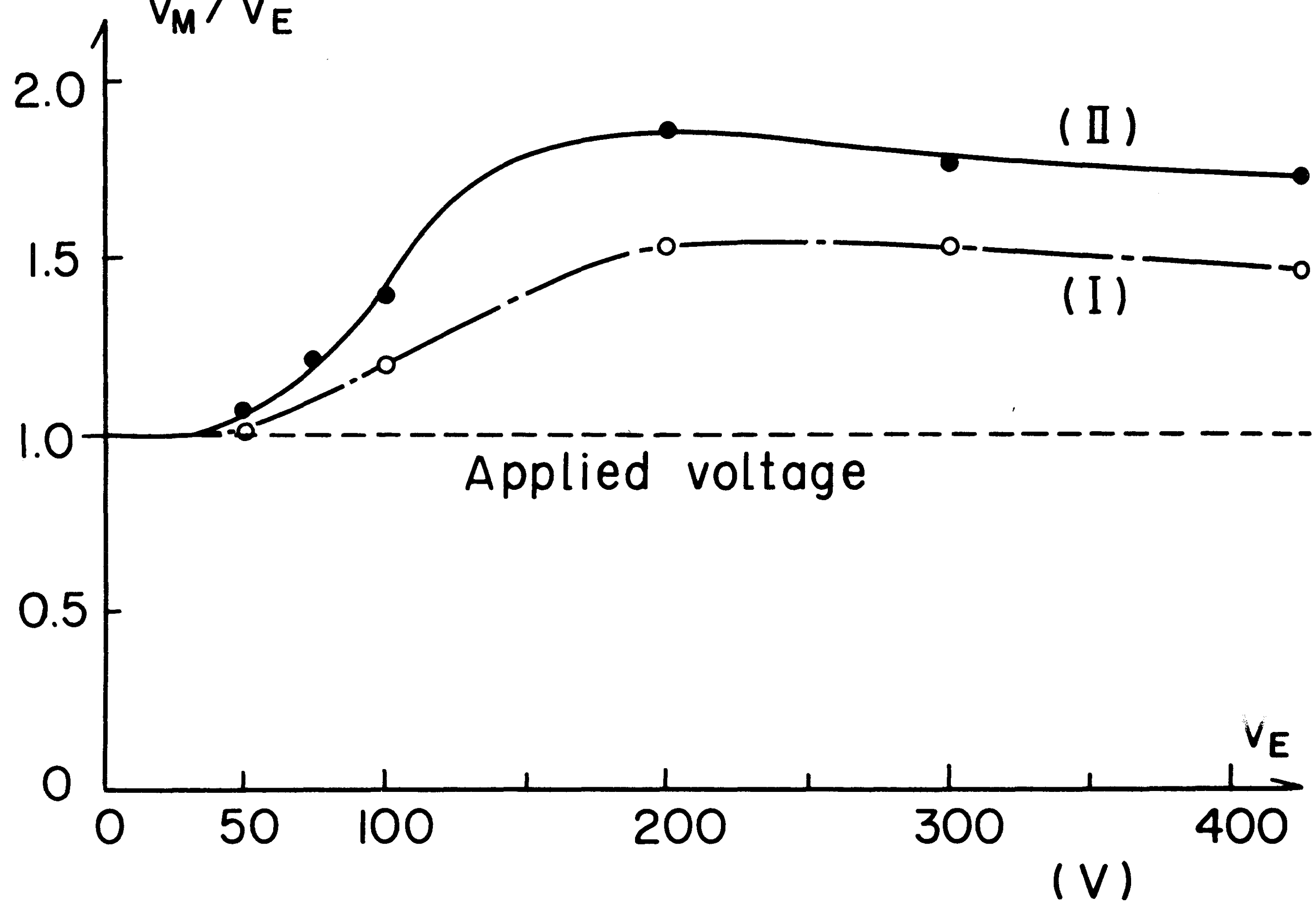

Fig.14

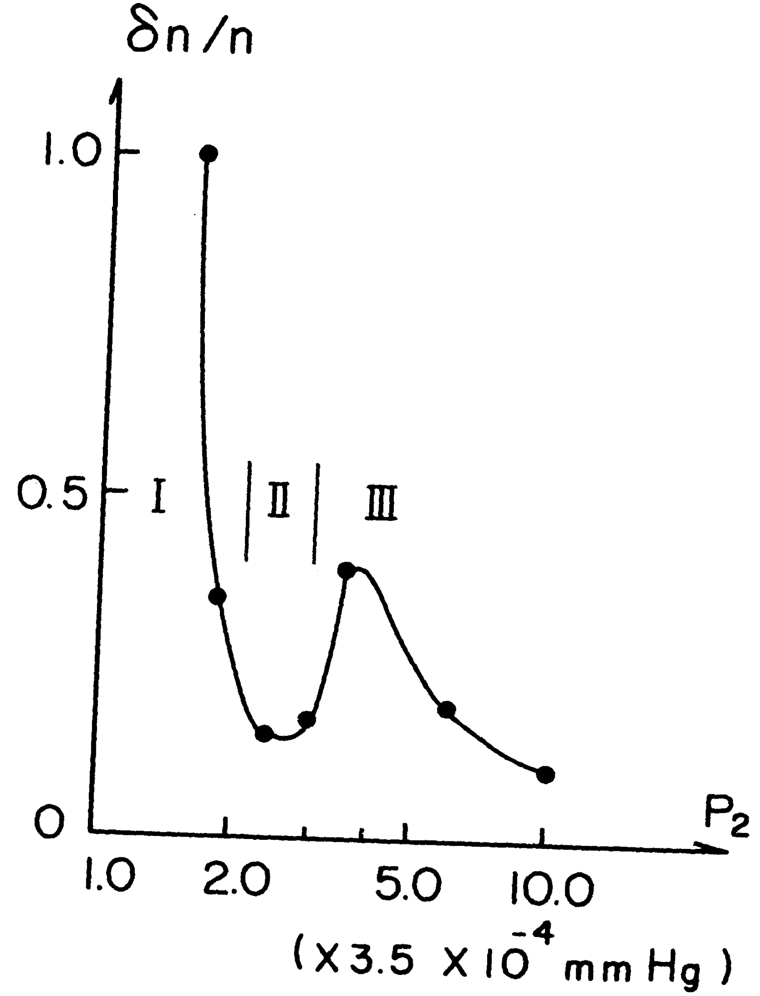

Fig. 15

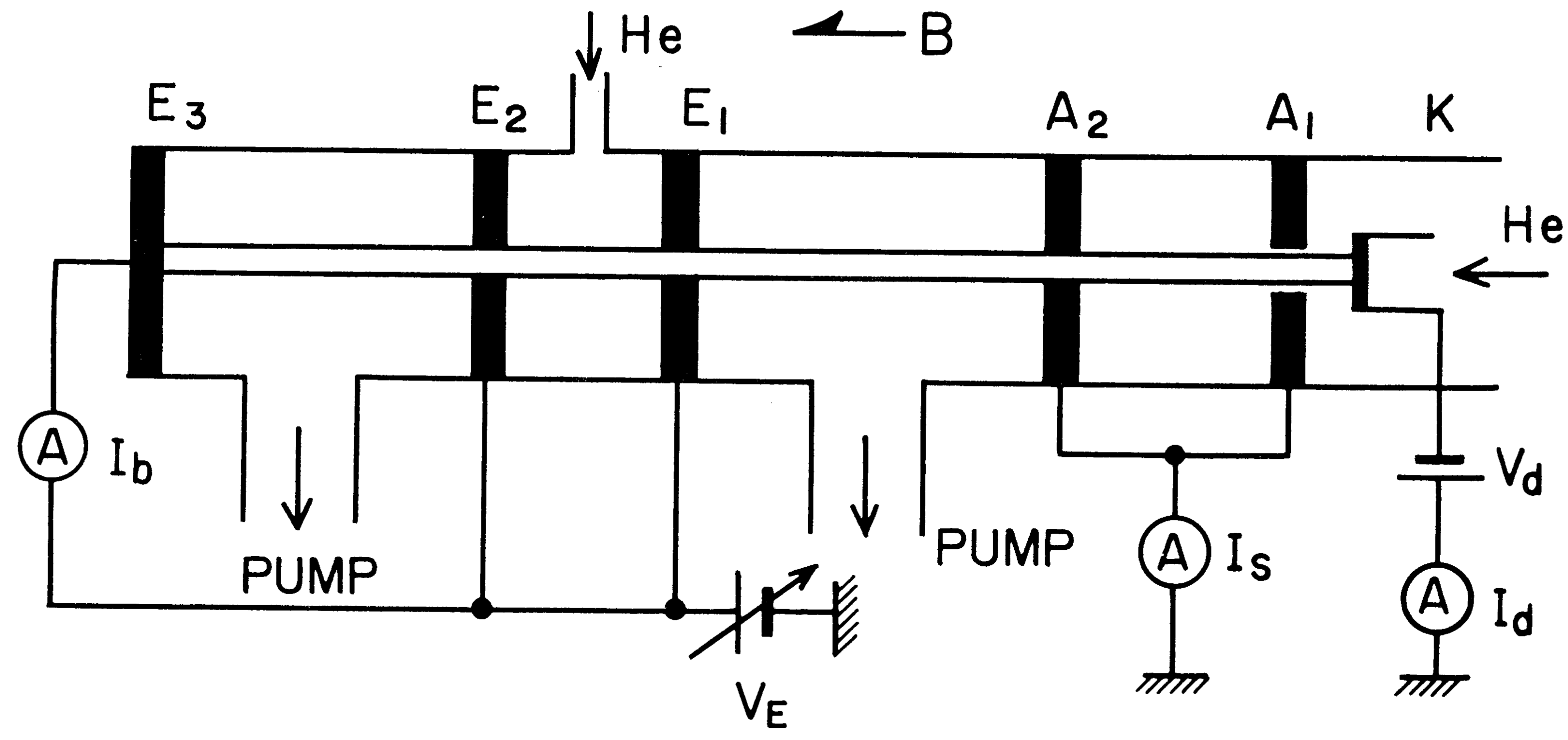

Fig.16

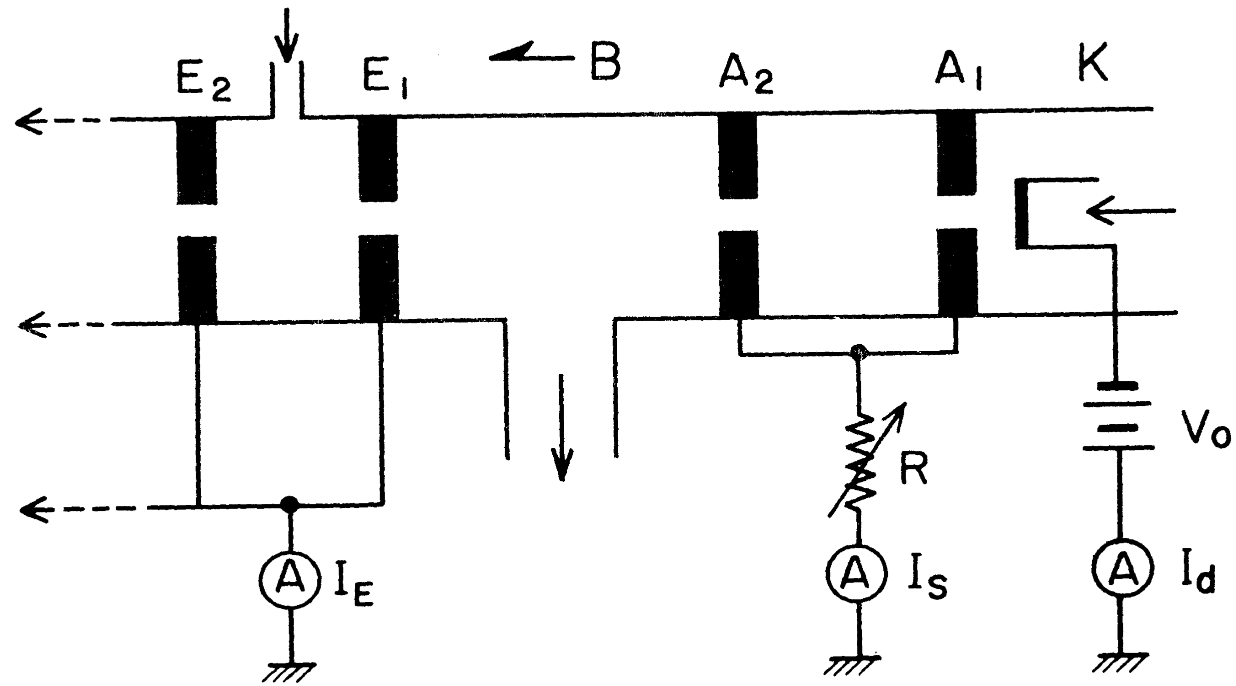

Fig.17